Online ISSN 1848-3380, Print ISSN 0005-1144
ATKAFF 56(1), 9–20(2015)

Paolo Pierro, Concepción A. Monje, Nicolas Mansard, Philippe Souères, Carlos Balaguer

Open Solution for Humanoid Attitude Estimation through Sensory Integration and Extended Kalman Filtering

DOI 10.7305/automatika.2015.04.593
UDK 681.532.8.015.42.015.44:007.52; 004.896

Original scientific paper

In this paper an Extended Kalman Filter (EKF) is used in order to estimate the real state of a humanoid robot (HRP-2 robot in our case study) using the combination of the information coming from the encoders (kinematics) and from the Inertial Measurement Unit (IMU). The integration of the kinematic information into the Kalman filtering process allows a good estimation of the attitude and reduces the complexity of the problem to the use of simple kinematic transformations, even considering the existence of accelerations and mechanical flexibilities in the robot. The EKF estimator presented here is an open solution directly applicable to any humanoid robot, which is the main contribution of our approach. Experimental results are given showing the good performance of the method.

Key words: Humanoid robot, Attitude estimation, Kalman filtering, Sensor integration, Kinematics simplicity

Otvoreno rješenje za estimaciju položaja humanoidnog robota integracijom senzora i proširenim Kalmanovim filtrom. U ovome članku koristi se prošireni Kalmanov filtar (EKF) za estimaciju stanja humanoidnog robota (HRP-2 robot) kombiniranjem informacija iz enkodera (kinematika) i inercijalne mjerne jedinice (IMU). Integracijom kinematičkih informacija u proces Kalmanovog filtra ostvaruje se dobra estimacija položaja i smanjenje složenosti problema jednostavnim kinematičkim transformacijama, čak i u slučaju postojanja akceleracija te mehaničkih savijanja robota. EKF predstavljen u ovome članku otvoreno je rješenje primjenjivo na bilo kojem humanoidnom robotu, što je i glavni doprinos predloženog pristupa. Ekperimentalni rezultati pokazuju dobro ponašanje predložene metode.

Ključne riječi: humanoidni robot, estimacija položaja, Kalmanov filtar, integracija senzora, kinematička jednostavnost

1 INTRODUCTION

One fundamental requisite for the control of a humanoid is having a good state estimation of the robot. Typically the states comprise positions, velocities and orientations. Unlike classical robotics, where position and orientation can be calculated using kinematic algorithms from a fixed base, in mobile robotics such a task is more complex. In particular, for the case of humanoid robots, the state estimation is important in order to detect the balance of the robot.

The robot's orientation with respect to the gravity vector or with respect to the world frame is referred to as attitude. For the balance control the attitude can be described by the roll and pitch angles [1]. Normally, the attitude estimation is achieved by the integration of several sensors, such as gyroscopes, inclinometers and accelerometers onboard the robot. This allows self-contained methods to estimate the attitude [2], [3]. Other measurements from external references, such as fixed cameras or updates from Global Position System (GPS) satellites, may not be relied on due to the potential for occlusion, sensor eccentricities, and the extended ranges of operation needed for some types of faster locomotion robots, such a galloping ones [4].

The attitude may be calculated using only the gyro output and integrating it. The problem is that the gyros measurements have usually significant noise, which may entail a great drift. Consequently, an absolute reference of the attitude can be obtained through the use of accelerometers, which provide the orientation with respect to the gravity vector. However, these are also quite sensitive to noise and, in addition, to the translational acceleration, which is usually considered as an additional noise component.

Even if the attitude estimation is a classical problem in mobile wheeled robotics [5], [6] and unmanned aerial vehicles (UAV) [7], [8], [9], several researchers have extended

such techniques to legged locomotion [10], [11], [12], [13], [14].

On the other hand, it is a fact that the body motion for walking robots is inherently three-dimensional, making most kinematic representations nonlinear. Many researchers face this problem using Extended Kalman Filters [15], [16], [17]. For instance, Rehbinder and Hu have previously designed an algorithm [18] for fusing inclinometer and gyro data assuming low translational accelerations, which may not be very realistic for a walking robot. Successively, they have provided an algorithm consisting of two modes: one when accelerations are low and the other when these are high [13]. More recent works are [19], [20], where the approach is the use of extended Kalman filters for three-dimensional pose estimation.

In this paper an open solution based on the Extended Kalman Filter (EKF) is used in order to estimate the real state of the humanoid robot HRP-2 (Fig. 1) using the combination of the information coming from the encoders (kinematics) and from the Inertial Measurement Unit (IMU). The integration of the kinematic information into the Kalman filtering process is one of our main approaches, allowing a good estimation of the attitude and reducing the complexity of the problem to the use of simple kinematic transformations. The scheme for the robot's state estimation is presented in Fig. 2, where:

ω is the gyroscope measurement.

a is the accelerometer measurement.

q_a is the angles position vector read by encoders.

q_p is the estimation of passive degrees of freedom (DOF), representing the mechanical flexibility.

R_c is the orientation estimation provided by the kinematics.

ω_c is the angular velocity estimation provided by the kinematics.

a_c is the linear acceleration estimation provided by the kinematics.

x is the vector containing information about the robot's attitude and state estimations.

In order to validate our solution, the proposed scheme has been experimentally tested on the humanoid robot HRP-2 and a comparison of the results with those obtained using OpenHRP estimator and a motion capture system is presented.

Regarding OpenHRP [21], it is a virtual humanoid robot platform (simulator) with a compatible humanoid

Fig. 1. HRP-2 robot

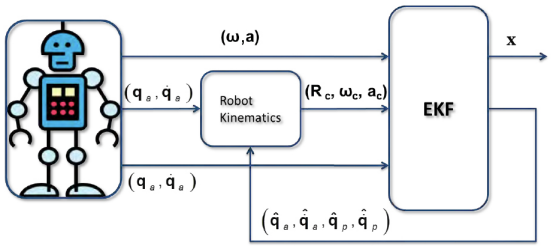

Fig. 2. Attitude estimation scheme

robot, in this case HRP-2. The software and hardware of this humanoid robot have been developed by Honda R&D and are provided to the OpenHRP architecture as a black box. The robot's controllers can be developed on the simulator and migrated into the hardware without any modification.

It is not clearly known how OpenHRP estimates the robot's attitude, since it is a closed system and not accessible for research, as can be seen from the short bibliography available on this specific topic. On the contrary, the EKF estimator presented in this work is a solution directly applicable to any humanoid robot. It is in that sense that we consider our proposal as 'open'.

The rest of the paper is organized as follows. Section 2 introduces the attitude representation and the derivative of the rotation matrix. Section 3 presents a solution for the fusion of sensors estimations. Section 4 details the EKF approach for the attitude estimation. Estimations obtained without and with consideration of accelerations are presented in Sections 5 and 6, respectively. Finally, some concluding remarks are given in Section 7.

2 ROBOT'S MODEL

2.1 Attitude representation

For the attitude representation in our system, the reference frames shown in Fig. 3 are used, where:

- $\mathscr{W}$ is an inertial world-fixed frame, with axis y_w pointing East and axis z_w pointing upward;
- $\mathscr{B}$ is a body-fixed frame attached to the sensor system (IMU) in the chest of the robot, with axis x_b pointing at the forward direction of the robot and z_b pointing upward. See Fig. 4 and Fig. 5 to identify the IMU location in the chest, at a distance of $0.469m$ from the robot's waist, and note that the reference system $\mathscr{B}$ in Fig. 3 is coincident with the reference system attached to the IMU in Fig. 4.

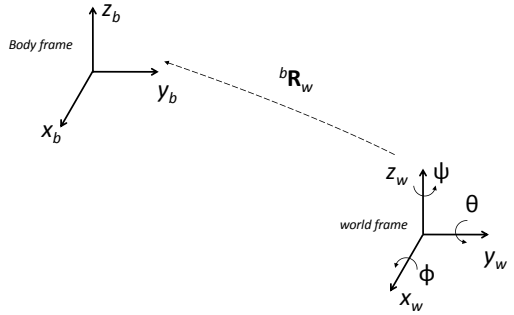

Fig. 3. Reference frames

We can define the rotation $\mathbf{R}$ as an orthogonal rotation matrix, element of the Spacial Orthogonal group $SO(3) \subset \mathbb{R}^{3\times3}$

$$SO(3) = \{\mathbf{R} \in \mathbb{R}^{3\times3} : \mathbf{R}^T\mathbf{R} = \mathbf{I}, det(\mathbf{R}) = 1\} \quad (1)$$

Therefore, ${}^a\mathbf{R}_b$ denotes the rotation matrix of frame b with respect to frame a, that is, $\mathbf{p}^b = {}^a\mathbf{R}_b\mathbf{p}^a$.

A minimal representation of the orientation of a frame with respect to another can be obtained by using a set of three angles (Euler angles). In this work we will use the Roll-Pitch-Yaw standard. In this case, the roll (ϕ), pitch (θ) and yaw (ψ) angles, expressed in frame $\mathscr{W}$, represent rotations defined with respect to a fixed frame.

If $\mathbf{R}_Z(\psi)$ is the rotation along axis z_w, $\mathbf{R}_Y(\theta)$ is the rotation along axis y_w, and $\mathbf{R}_X(\phi)$ is the rotation along axis x_w, such orientation can be defined as [22]:

$$\begin{aligned}\mathbf{R}_{RPY} &= \mathbf{R}_Z(\psi)\mathbf{R}_Y(\theta)\mathbf{R}_X(\phi) = \\ &= \begin{bmatrix} c_\theta c_\psi & c_\psi s_\theta s_\phi - c_\phi s_\psi & s_\phi s_\psi + c_\phi c_\psi s_\theta \\ c_\theta s_\psi & c_\phi c_\psi + s_\theta s_\phi s_\psi & c_\phi s_\theta s_\psi - c_\psi s_\phi \\ -s_\theta & c_\theta s_\phi & c_\theta c_\phi \end{bmatrix}\end{aligned} \quad (2)$$

If we use such a matrix to describe the orientation of frame $\mathscr{B}$ with respect to the reference frame $\mathscr{W}$, this matrix will also be the transformation matrix of the vector coordinates from frame $\mathscr{B}$ into the coordinates of the same vector in frame $\mathscr{W}$, that is, ${}^w\mathbf{R}_b = \mathbf{R}_{RPY}$.

Besides, for a rotation matrix $\mathbf{R}$, it is possible to define the matrix $\mathbf{S}$ as

$$\mathbf{S}(\omega(t)) = \dot{\mathbf{R}}(t)\mathbf{R}(t) \quad (3)$$

where the vector $\omega(t)$ denotes the angular velocity of frame $\mathbf{R}(t)$ with respect to the reference frame at time t.

It is possible to easily show that the following relations hold [22]:

$$\begin{aligned}\mathbf{S}(\omega) + \mathbf{S}^T(\omega) &= \mathbf{O} \\ \mathbf{S}(\mathbf{R}_0\omega) &= \mathbf{R}_0\mathbf{S}(\omega)\mathbf{R}_0^T\end{aligned} \quad (4)$$

2.2 Kinematic model of the robot

The kinematic model of the humanoid robot HRP-2 is presented here, detailing the coordinates systems and joint variables for the robot's torso and legs, and including the kinematics for the flexible ankle, whose effects will be considered later.

In Fig. 4, Fig. 5 and Fig. 6 the kinematics of the robot's torso, its dimensions and its Denavit-Hartenberg (DH) parameters are shown, respectively (note that the IMU reference system is coincident with the body-fixed frame $\mathscr{B}$). As can be seen from Fig. 5, where the dimensions of the torso are given, the IMU system is placed at a distance of $Waist\_Link2 + Torso\_Link2 = 0.469m$ from the waist.

Kinematics and DH parameters for the floating and standing leg and for the flexible ankle are also presented from Fig. 7 to Fig. 12. The dimensions of legs are presented in Fig. 13.

Knowing these kinematic models and their DH parameters and taking the angular position measurements from the encoders as an input, and through the direct application of the direct kinematics theory, we can easily reach an estimation of the orientation of frame $\mathscr{B}$ with respect to the reference frame $\mathscr{W}$ (R_c in Fig. 2), an estimation of the angular velocities of the body frame relative to the inertial frame (ω_c in Fig. 2) and an estimation of the linear acceleration of the body frame relative to the inertial frame (a_c in Fig. 2).

2.3 Fusion of sensors estimations

In this study we provide a solution to fusing data from a 3-axis rate gyro and a 3-axis accelerometer that will provide stable estimates of the robot's attitude.

The 3-axis gyroscope provides the angular velocities of the body frame relative to the inertial frame, expressed in the body-fixed frame. If the measured angular rates were

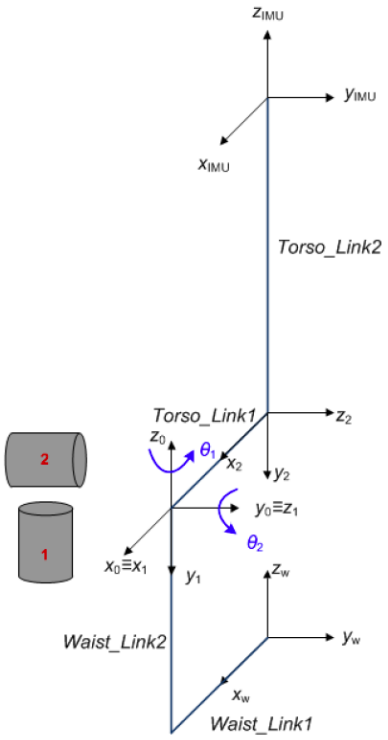

Fig. 4. Kinematic model for the robot's torso

Name	Symbol	Length [m]
Waist	Waist_Link1	0.032
	Waist_Link2	0.351
Torso	Torso_Link1	0.130
	Torso_Link2	0.118

Fig. 5. Dimensions of the robot's torso

Name	Joint type	number	a_i	α_i	d_i	θ_i
Torso	Yaw	1	0	$-\frac{\pi}{2}$	0	θ_1
	Pitch	2	$-$Torso_Link1	0	0	θ_2

Fig. 6. DH parameters for the robot's torso

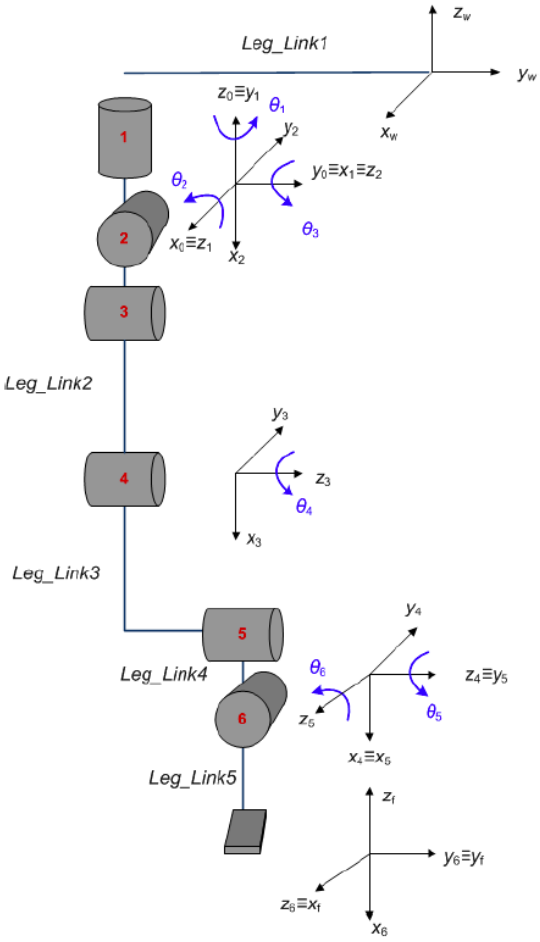

Fig. 7. Kinematic model for the robot's floating leg

Name	Joint type	number	a_i	α_i	d_i	θ_i
Right hip	Yaw	1	0	$\frac{\pi}{2}$	0	$\theta_1+\frac{\pi}{2}$
	Roll	2	0	$-\frac{\pi}{2}$	0	$\theta_2-\frac{\pi}{2}$
	Pitch	3	Leg_Link2	0	0	θ_3
Right knee	Pitch	4	Leg_Link3	0	Leg_Link4	θ_4
Right ankle	Pitch	5	0	$\frac{\pi}{2}$	0	θ_5
	Roll	6	Leg_Link5	0	0	θ_6

Fig. 8. DH parameters for the robot's floating leg

perfect, it would be sufficient to integrate these measurements using equation (3) to provide the orientation matrix $\mathbf{R}$. However, due to openloop integrations, any bias on gyroscopic measurements lead to an error on the attitude prediction, which grows to infinity. This phenomena is known as gyroscopic drift.

To take into account on-line estimation of gyroscope bias, we consider the model of gyroscopic measurements given by

$$\omega_m = \omega + \omega_0 + \omega_n \tag{5}$$

where ω is the real angular velocity and ω_0 is the gyroscope bias, which depends on the temperature. Many low cost IMU are now internally compensated in temperature, and as a result, ω_0 oscillates slowly around a constant average value [9], reason why we consider it to be constant with the time. The term ω_n is a Gaussian white noise.

The 3-axis accelerometer measures the difference between the inertial forces and gravity forces, expressed in frame $\mathscr{B}$. The model of the accelerometer is given by

$$\mathbf{a}_m = {}^b\mathbf{R}_w\,(\mathbf{a}-\mathbf{g}) + \mathbf{a}_0 + \mathbf{a}_n \tag{6}$$

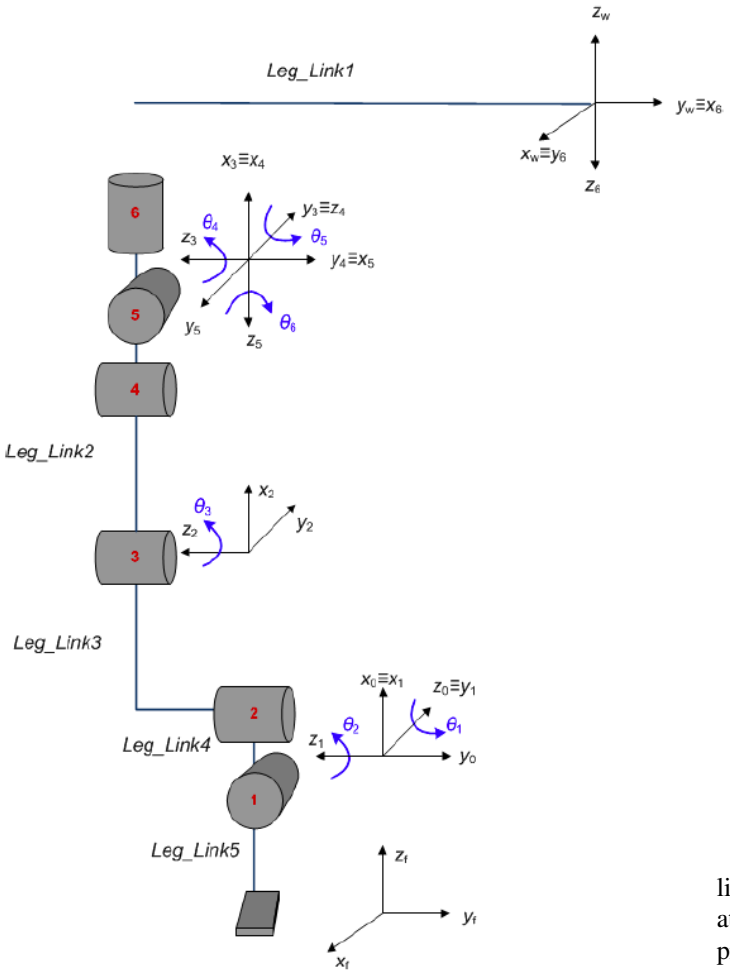

Fig. 9. Kinematic model for the robot's standing leg

Name	Joint type	number	a_i	α_i	d_i	θ_i
Right ankle	Roll	1	0	$\frac{\pi}{2}$	0	θ_1
	Pitch	2	Leg_Link3	0	Leg_Link4	θ_2
Right knee	Pitch	3	Leg_Link2	0	0	θ_3
Right hip	Pitch	4	0	$-\frac{\pi}{2}$	0	θ_4
	Roll	5	0	$-\frac{\pi}{2}$	0	$\theta_5+\frac{\pi}{2}$
	Yaw	6	Leg_Link1	0	0	θ_6

Fig. 10. DH parameters for the robot's standing leg

where $\mathbf{a}$ is the acceleration in the frame $\mathscr{W}$, $\mathbf{g}$ is the gravity vector, $\mathbf{a}_0$ is a bias and $\mathbf{a}_n$ is a Gaussian white noise.

If measurements were absolutely reliable, pitch and roll of the vehicle could be directly deduced from the accelerometers, working as inclinometers in that case. However, readings from accelerometers are very noisy and very sensitive to the vibratory environment surrounding the IMU. Furthermore, if for any reason the robot acquires a non negligible absolute acceleration in the inertial frame, the attitude provided by accelerometers will no more be reliable. Therefore, it is important in practice to correlate the attitude measured by the accelerometers and the attitude predicted by integrating the gyroscopic measurements to provide a correct attitude estimation.

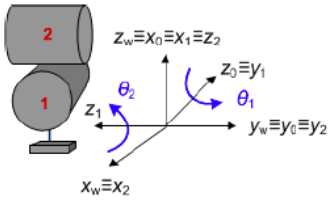

Fig. 11. Kinematic model for the flexible ankle

Name	Joint type	number	a_i	α_i	d_i	θ_i
Flexibility	Roll	1	0	$\frac{\pi}{2}$	0	θ_1
	Pitch	2	0	$-\frac{\pi}{2}$	0	$\theta_2-\frac{\pi}{2}$

Fig. 12. DH parameters for the flexible ankle

Name	Symbol	Length [m]
Waist	Leg_Link1	0.06
Femur	Leg_Link2	0.3
Tibia	Leg_Link3	0.3
Patella	Leg_Link4	0.035
Astragalus	Leg_Link5	0.105

Fig. 13. Dimensions of the robot's legs

If $\mathbf{p}=(x,y,z)$ is an arbitrary point, we will denote $\mathbf{p}^w$ when expressed in frame $\mathscr{W}$ and $\mathbf{p}^b$ when expressed in frame $\mathscr{B}$, *i.e.*:

$$\mathbf{p}^w = {}^w\mathbf{o}_b + {}^w\mathbf{R}_b\mathbf{p}^b \tag{7}$$

where ${}^w\mathbf{o}_b$ is the vector describing the origin of frame $\mathscr{B}$ with respect to frame $\mathscr{W}$.

This equation can be rewritten as

$$\mathbf{p}^b = {}^w\mathbf{R}_b^T\left(\mathbf{p}^w - {}^w\mathbf{o}_b\right) \tag{8}$$

Using equation (3), it is possible to write

$${}^w\dot{\mathbf{R}}_b = \mathbf{S}(\omega^w){}^w\mathbf{R}_b \tag{9}$$

which can be rewritten using equation (4) as

$${}^w\dot{\mathbf{R}}_b^T = -{}^w\mathbf{R}_b^T\mathbf{S}(\omega^w) = {}^w\mathbf{R}_b^T\mathbf{S}({}^w\mathbf{R}_b\omega^b) = -\mathbf{S}(\omega^b){}^w\mathbf{R}_b^T \tag{10}$$

The kinematics of a rigid body is given by

$$\begin{cases} {}^w\ddot{\mathbf{o}}_b = \mathbf{a} \\ {}^w\dot{\mathbf{R}}_b^T(t) = -\mathbf{S}\left(\omega^b(t)\right){}^w\mathbf{R}_b^T(t) \end{cases} \tag{11}$$

where $\mathbf{S}(\omega^b)$ is a skew-symmetric matrix defined as

$$\mathbf{S}(\omega^b) = \begin{pmatrix} 0 & -\omega_z & \omega_y \\ \omega_z & 0 & -\omega_x \\ -\omega_y & \omega_x & 0 \end{pmatrix} \tag{12}$$

where ω_i is the components of the angular velocity expressed in frame $\mathscr{B}$.

So, we can write the equation for the rotation as

$${}^b\dot{\mathbf{R}}_w = -\mathbf{S}(\omega^b){}^b\mathbf{R}_w \tag{13}$$

Taking the time-derivative of (2) and comparing with (13), for the roll and pitch angles we get

$$\dot{\mathbf{x}} = \begin{bmatrix} \dot{\phi} \\ \dot{\theta} \end{bmatrix} = \begin{bmatrix} 1 & \sin(\phi)\tan(\theta) & \cos(\phi)\tan(\theta) \\ 0 & \cos(\phi) & \sin(\phi) \end{bmatrix} \begin{bmatrix} \omega_x \\ \omega_y \\ \omega_z \end{bmatrix} \tag{14}$$

where $\mathbf{x}$ is the state vector. If we consider the real acceleration as a disturbance and the gravity vector $\mathbf{g}$ as an entity to measure, we can use the accelerometer as an attitude sensor [6]. So, we have

$$\mathbf{a}_m \simeq -{}^b\mathbf{R}_w\mathbf{g} \tag{15}$$

3 EXTENDED KALMAN FILTERING APPROACH

The EKF evaluates the partial derivatives at the estimated state vector value and uses the full nonlinear functions on the estimate itself. The EKF assumes a model in the discrete form [14]:

$$\begin{aligned} \mathbf{x}(k+1) &= f(\mathbf{x}(k), \mathbf{u}(k)) + \nu_k \\ \mathbf{y}(k) &= h(\mathbf{x}(k)) + \mathbf{w}_k \end{aligned} \tag{16}$$

The prediction phase will be

$$\mathbf{x}_{k+1|k} = f(\mathbf{x}_k, \mathbf{u}_k) \tag{17}$$

The predicted covariance is

$$\mathbf{P}_{k+1|k} = \mathbf{F}_k\mathbf{P}_{k|k}\mathbf{F}_k^T + \mathbf{F}_\nu\mathbf{Q}\mathbf{F}_\nu^T \tag{18}$$

where $\mathbf{F}$ is the Jacobian matrix such that:

$$\mathbf{F} = \frac{\partial f}{\partial \mathbf{x}} \tag{19}$$

The measurement update:

$$\mathbf{x}_{k+1|k+1} = \mathbf{x}_{k+1|k} + \mathbf{K}_{k+1|k}(h(\mathbf{x}_k) - \mathbf{y}_k) \tag{20}$$

$$\mathbf{P}_{k+1|k+1} = \mathbf{P}_{k+1|k} + \mathbf{K}_{k+1|k}(h(\mathbf{x}_k) - \mathbf{y}_k)\mathbf{F}_k\mathbf{P}_{k|k}\mathbf{F}_k^T + \mathbf{Q} \tag{21}$$

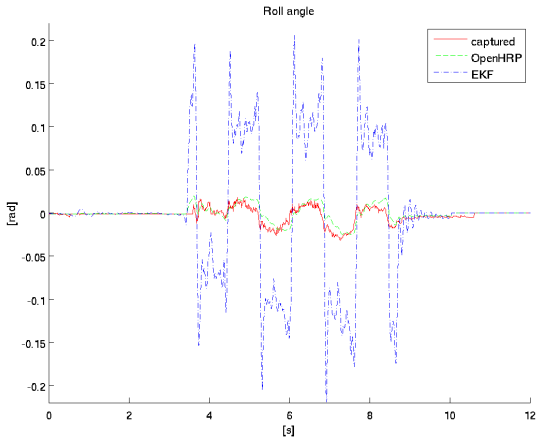

Fig. 14. Estimation of roll angle with $\sigma(a_n) = 0.1\mathbf{I}[m/s^2]$

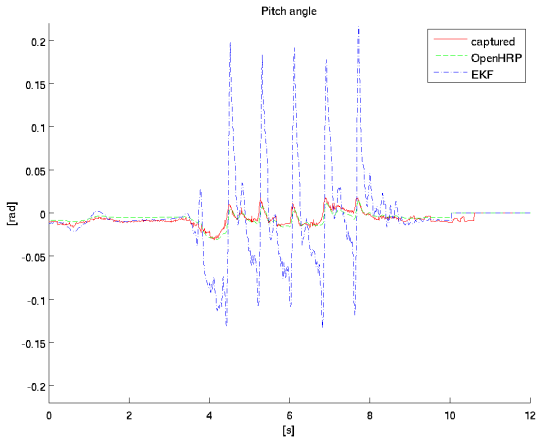

Fig. 15. Estimation of pitch angle with $\sigma(a_n) = 0.1\mathbf{I}[m/s^2]$

4 ESTIMATION WITHOUT CONSIDERING REAL ACCELERATION

In the ideal case, when the accelerations are low enough to be considered zero, the results are presented in the following figures. The real pitch/roll angles (estimated by a motion capture system) are compared with the OpenHRP estimation and the EKF estimation.

The following video shows the real experiment with HRP-2 robot, carried out at the facilities of the LASS Laboratory in Toulouse, France:

`youtube.com/watch?v=x8_G2YIapLI&feature=youtu.be`

In Fig. 14 and Fig. 15 the accelerometer noise standard deviation has been fixed to $0.1\mathbf{I}[m/s^2]$, to $\mathbf{I}[m/s^2]$ in Fig. 16 and Fig. 17, and to $10\mathbf{I}[m/s^2]$ in Fig. 18 and Fig. 19.

Figure 20 and Fig. 21 show the results of the estimations of the roll and pitch angles while the robot is on the crane and subjected to external pushing forces.

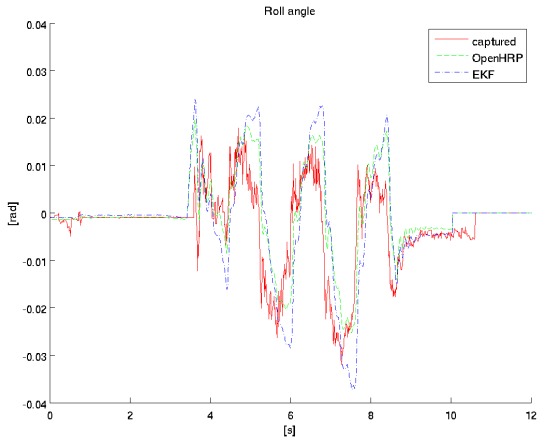

Fig. 16. Estimation of roll angle with $\sigma(a_n) = \mathbf{I}[m/s^2]$

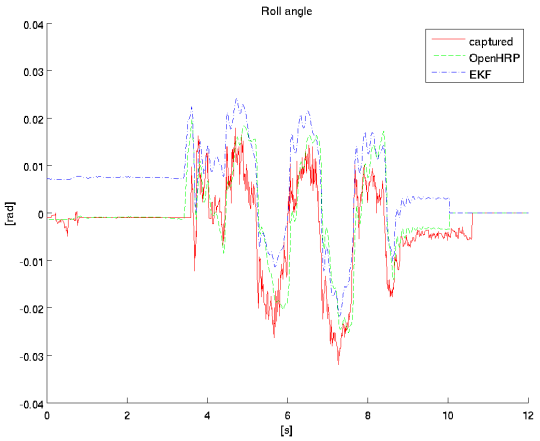

Fig. 18. Estimation of roll angle with $\sigma(a_n) = 10\mathbf{I}[m/s^2]$

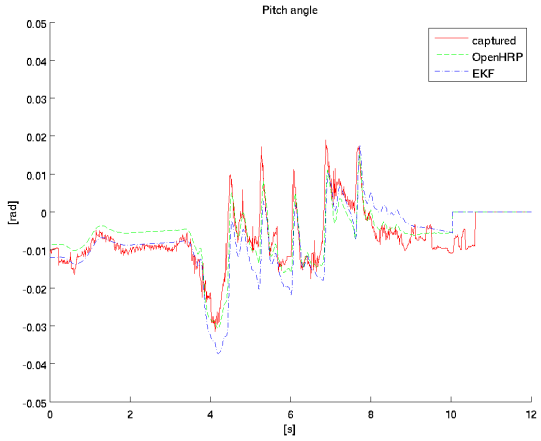

Fig. 17. Estimation of pitch angle with $\sigma(a_n) = \mathbf{I}[m/s^2]$

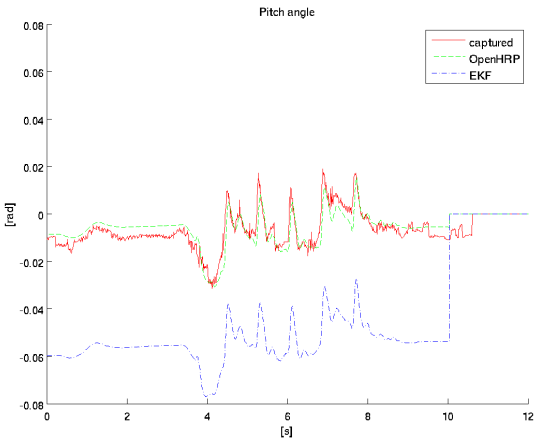

Fig. 19. Estimation of pitch angle with $\sigma(a_n) = 10\mathbf{I}[m/s^2]$

5 ESTIMATION USING REAL ACCELERATION AND MECHANICAL FLEXIBILITY

The flexibility in the ankle can be treated as a pair of passive joints: $\mathbf{q}_p$ is the position vector of the robot flexibility in the ankle (pitch and roll). The position vector, of dimension n, of the active robot links (from the standing foot up to the IMU) is denoted as $\mathbf{q}_a$. As can be seen from Section 2, where the kinematics of the robot has been described, in our case $n = 8$ (see Fig. 4 and Fig. 9). In a compact form the position vector of the joints is

$$\mathbf{q} = \begin{bmatrix} \mathbf{q}_p \\ \mathbf{q}_a \end{bmatrix} \tag{22}$$

The size of such vector is $n_p = n + 2$. The robot's state vector is selected to be

$$\mathbf{x} = \begin{bmatrix} \mathbf{q} \\ \dot{\mathbf{q}} \\ \ddot{\mathbf{q}} \\ \omega_0 \end{bmatrix} = \begin{bmatrix} \mathbf{q}_p \\ \mathbf{q}_a \\ \dot{\mathbf{q}}_p \\ \dot{\mathbf{q}}_a \\ \ddot{\mathbf{q}}_p \\ \ddot{\mathbf{q}}_a \\ \omega_0 \end{bmatrix} \tag{23}$$

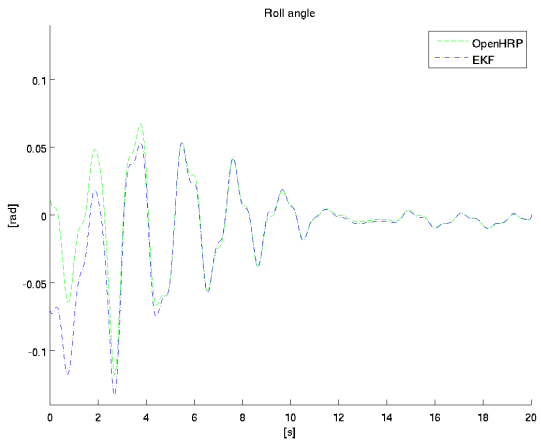

Fig. 20. Estimation of roll angle with $\sigma(a_n) = \mathbf{I}[m/s^2]$. Robot on the crane and subjected to external pushing forces

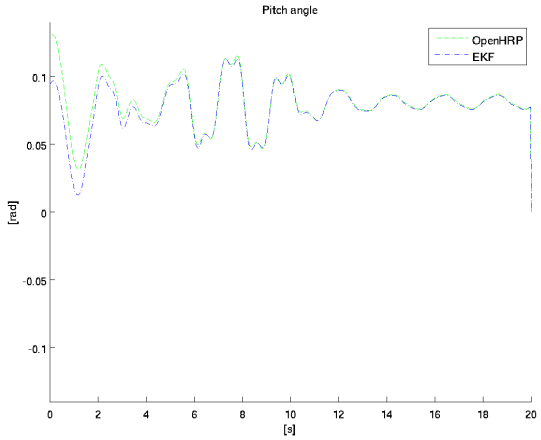

Fig. 21. Estimation of pitch angle with $\sigma(a_n) = \mathbf{I}[m/s^2]$. Robot on the crane and subjected to external pushing forces

So, the state transition will be

$$\begin{bmatrix} \mathbf{q}_p(k+1) \\ \mathbf{q}_a(k+1) \\ \dot{\mathbf{q}}_p(k+1) \\ \dot{\mathbf{q}}_a(k+1) \\ \ddot{\mathbf{q}}_p(k+1) \\ \ddot{\mathbf{q}}_a(k+1) \\ \omega_0(k+1) \end{bmatrix} =$$

$$\begin{bmatrix} \mathbf{1} & \mathbf{0} & \mathbf{T_s} & \mathbf{0} & \mathbf{0} & \mathbf{0} & \mathbf{0} \\ \mathbf{0} & \mathbf{1} & \mathbf{0} & \mathbf{Ts} & \mathbf{0} & \mathbf{0} & \mathbf{0} \\ \mathbf{0} & \mathbf{0} & \mathbf{1} & \mathbf{0} & \mathbf{0} & \mathbf{0} & \mathbf{0} \\ \mathbf{0} & \mathbf{0} & \mathbf{0} & \mathbf{1} & \mathbf{0} & \mathbf{Ts} & \mathbf{0} \\ \mathbf{0} & \mathbf{0} & \mathbf{0} & \mathbf{0} & \mathbf{1} & \mathbf{0} & \mathbf{Ts} \\ \mathbf{0} & \mathbf{0} & \mathbf{0} & \mathbf{0} & \mathbf{0} & \mathbf{1} & \mathbf{0} \\ \mathbf{0} & \mathbf{0} & \mathbf{0} & \mathbf{0} & \mathbf{0} & \mathbf{0} & \mathbf{1} \end{bmatrix} \begin{bmatrix} \mathbf{q}_p(k) \\ \mathbf{q}_a(k) \\ \dot{\mathbf{q}}_p(k) \\ \dot{\mathbf{q}}_a(k) \\ \ddot{\mathbf{q}}_p(k) \\ \ddot{\mathbf{q}}_a(k) \\ \omega_0(k) \end{bmatrix} + \begin{bmatrix} \mathbf{n}_{p,p} \\ \mathbf{n}_{a,p} \\ \mathbf{n}_{p,v} \\ \mathbf{n}_{a,v} \\ \mathbf{n}_{p,a} \\ \mathbf{n}_{a,a} \\ \mathbf{n}_{\omega} \end{bmatrix} \tag{24}$$

where T_s is the sampling time.

The measurements will be defined by the nonlinear system

$$\mathbf{y} = \begin{bmatrix} \mathbf{a}_b \\ \omega_b \\ \dot{\mathbf{q}}_e \\ \mathbf{q}_e \end{bmatrix} = \begin{bmatrix} {}^b\mathbf{R}_w(\mathbf{a}-\mathbf{g}) \\ \omega + \omega_0 \\ \dot{\mathbf{q}}_a \\ \mathbf{q}_a \end{bmatrix} + \begin{bmatrix} \mathbf{a}_n \\ \omega_n \\ \mathbf{q}_n \\ \mathbf{q}_{n,d} \end{bmatrix} \tag{25}$$

where $\mathbf{q}_e$ is the position read by the encoders.

Now, defining $\mathbf{J}_P$ as the $(3 \times n)$ matrix relating the contribution of the joint velocities $\dot{\mathbf{q}}$ to the linear velocity and $\mathbf{J}_O$ as the $(3 \times n)$ matrix relating the contribution of the joint velocities $\dot{\mathbf{q}}$ to the angular velocity, it is possible to write

$$\mathbf{J}(\mathbf{q}) = \begin{bmatrix} \mathbf{J}_P(\mathbf{q}) \\ \mathbf{J}_O(\mathbf{q}) \end{bmatrix} \tag{26}$$

For $\mathbf{a}$ being the linear acceleration, we can write

$$\mathbf{a} = \mathbf{J}_P\ddot{\mathbf{q}} + \dot{\mathbf{J}}_P\dot{\mathbf{q}} = \mathbf{J}_P\ddot{\mathbf{q}} + \dot{\mathbf{q}}^T\mathbf{H}_P\dot{\mathbf{q}} \tag{27}$$

the Hessian matrix being denoted by $\mathbf{H}_P = \frac{\partial \mathbf{J}_P}{\partial \mathbf{q}}$.

Finally, (25) can be rewritten as

$$\mathbf{y} = \begin{bmatrix} \mathbf{a}_b \\ \omega_b \\ \dot{\mathbf{q}}_e \\ \mathbf{q}_e \end{bmatrix} =$$

$$\begin{bmatrix} {}^b\mathbf{R}_w(\mathbf{q})\left(\mathbf{J}_P(\mathbf{q})\ddot{\mathbf{q}} + \dot{\mathbf{q}}^T\mathbf{H}_P(\mathbf{q})\dot{\mathbf{q}} - \mathbf{g}\right) \\ \mathbf{J}_O(\mathbf{q})\dot{\mathbf{q}} + \omega_0 \\ \dot{\mathbf{q}}_a \\ \mathbf{q}_a \end{bmatrix} + \begin{bmatrix} \mathbf{a}_n \\ \omega_n \\ \mathbf{q}_n \\ \mathbf{q}_{n,d} \end{bmatrix} \tag{28}$$

For the sake of simplicity, matrix ${}^b\mathbf{R}_w$ will be denoted as $\mathbf{R}$. Writing the measurement function as

$$h(\mathbf{x}) = \begin{bmatrix} \mathbf{R}\left(\mathbf{J}_P\ddot{\mathbf{q}} + \dot{\mathbf{q}}^T\mathbf{H}_P\dot{\mathbf{q}} - \mathbf{g}\right) \\ \mathbf{J}_O\dot{\mathbf{q}} + \omega_0 \\ \dot{\mathbf{q}}_a \\ \mathbf{q}_a \end{bmatrix} \tag{29}$$

its Jacobian matrix can be written as

$$\mathbf{H} = \frac{\partial h}{\partial \mathbf{x}} = \begin{bmatrix} \mathbf{H_q} & \mathbf{H_{\dot{q}}} & \mathbf{H_{\ddot{q}}} & \mathbf{H_{\omega_0}} \end{bmatrix} \tag{30}$$

where

$$\mathbf{H_q} = \begin{bmatrix} \frac{\partial \mathbf{R}}{\partial \mathbf{q}} \left(\mathbf{J}_P \ddot{\mathbf{q}} + \dot{\mathbf{q}}^T \mathbf{H}_P \dot{\mathbf{q}} - \mathbf{g} \right) + \mathbf{R} \left(\mathbf{H}_P \ddot{\mathbf{q}} + \dot{\mathbf{q}}^T \mathbf{K}_P \dot{\mathbf{q}} \right) \\ \mathbf{H}_O \dot{\mathbf{q}} \\ \mathbf{0}_{2,n} \\ \mathbf{0}_{n,n} \\ \mathbf{0}_{2,n} \\ \mathbf{I}_n \end{bmatrix} \tag{31}$$

where $\mathbf{K}_P = \frac{\partial \mathbf{H}_P}{\partial \mathbf{q}}$ is the second-derivative of the Jacobian $\mathbf{J}_P$.

$$\mathbf{H}_{\dot{\mathbf{q}}} = \begin{bmatrix} \mathbf{R} \left(\mathbf{H}_P \dot{\mathbf{q}} + \dot{\mathbf{q}}^T \mathbf{H}_P \right) \\ \mathbf{J}_O \\ \mathbf{0}_{2,n} \\ \mathbf{I}_n \\ \mathbf{0}_{2,n} \\ \mathbf{0}_{n,n} \end{bmatrix} \tag{32}$$

$$\mathbf{H}_{\ddot{\mathbf{q}}} = \begin{bmatrix} \mathbf{R}\mathbf{J}_P \\ \mathbf{0}_{3,n+2} \\ \mathbf{0}_{n+2,n+2} \\ \mathbf{0}_{n+2,n+2} \end{bmatrix} \tag{33}$$

$$\mathbf{H}_{\omega_\mathbf{0}} = \begin{bmatrix} \mathbf{0}_{3,3} \\ \mathbf{I}_3 \\ \mathbf{0}_{n,3} \\ \mathbf{0}_{n,3} \end{bmatrix} \tag{34}$$

denoting $\mathbf{O}_{i,j}$ as the zero matrix of size $i \times j$ and $\mathbf{I}_i$ as the identity matrix of size $i \times i$.

The last part of the experimental test video referenced before shows the real experiment with HRP-2 robot during a standard forward walking. From Fig. 22 to Fig. 24 the results of the estimation during the walking are presented. The captured data is compared with the OpenHRP estimation and the EKF estimation. Finally, Fig. 25 presents an estimation of the flexibility in the robot's ankle.

It is important to remark that the comparison between the EKF with kinematics information and the EKF running in OpenHRP is made considering that the real robot's attitude is the one calculated through the Motion Capture System. Anyway, it is not clearly known how the OpenHRP estimates the robot's attitude, since it is a closed system and not accessible for research. On the contrary, our EKF estimator is an open solution directly applicable to any humanoid robot, which is the main contribution of our approach.

6 CONCLUSIONS

This paper has studied a major problem when dealing with the control of humanoid platforms: the attitude estimation. While most authors estimate the robot's attitude combining acceleration and gyroscope measurements

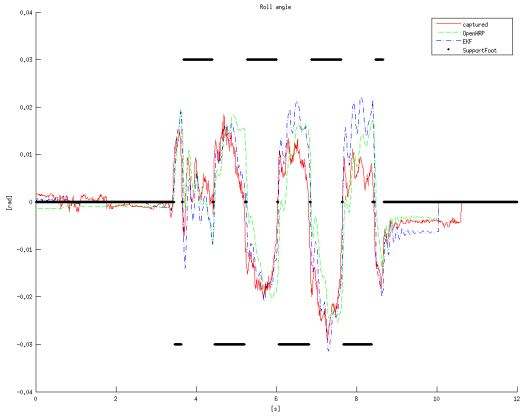

Fig. 22. Roll angle estimation during a standard forward walking

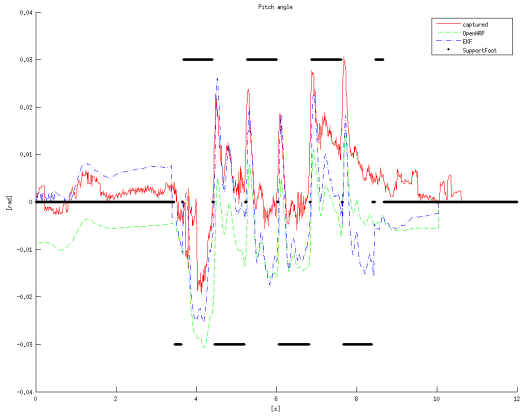

Fig. 23. Pitch angle estimation during a standard forward walking

through the use of EKF, in our approach the kinematics information is also integrated in order to improve the filtering. Using the information coming from the robot's encoders and simple kinematic transformations, this method allows obtaining a good estimation of the robot's attitude with respect to the world frame, even considering the existence of accelerations and mechanical flexibilities in the robot.

This method has been implemented on the humanoid robot HRP-2, comparing the results with the information obtained from the robot's inner stabilizer and showing the better performance of the proposed approach.

Other algorithms must be explored next, such as the particle filtering. A better performance may lie on the use of an n-states estimator, in which a different estimator is

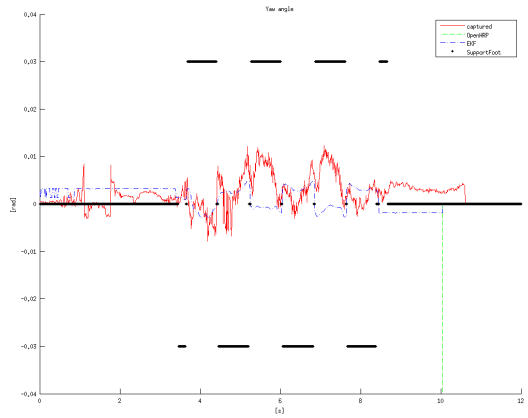

Fig. 24. Yaw angle estimation during a standard forward walking

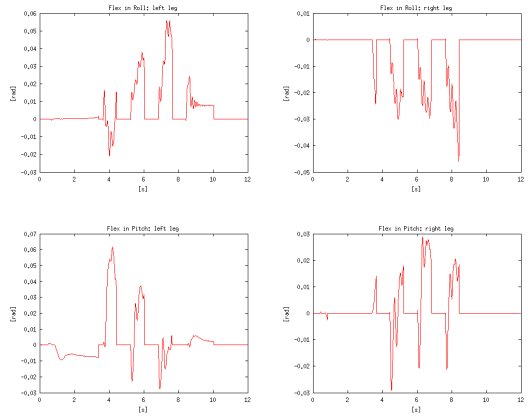

Fig. 25. Estimation of roll and pitch angles considering mechanical flexibilities in the ankle

used for each robot walking phase (single and double support).

ACKNOWLEDGEMENTS

We would like to acknowledge the support of LAAS-CNRS during the experimental tests with HRP-2 robot.

This work has been funded by the CICYT-MICINN Project Arcadia DPI2010-21047 and the Community of Madrid Project RoboCity2030 S2009/DPI-1559.

REFERENCES

[1] M. H. Raibert, "Legged robots that balance," *MIT Press series in Artificial Intelligence*, 1986.

[2] A. Chilian, H. Hirschmuller, and M. Gorner, "Multisensor data fusion for robust pose estimation of a six-legged walking robot," in *Proceedings of the 2011 IEEE/RSJ International Conference on Intelligent Robots and Systems, IROS 2011*, (San Francisco, California), pp. 2497–2504, September 2011.

[3] C. G. Bu, Z. W. Wu, C. Chen, and Y. Zhuang, "Review on state estimation technology of four-leg robot," in *Proceedings of the 5th IEEE International Conference on Cybernetics and Intelligent Systems and the 5th IEEE International Conference on Robotics, Automation and Mechatronics*, 2011.

[4] J. Farrel and M. Barth, *The Global Positioning System and Inertial Navigation*. McGraw-Hill, New York, 1999.

[5] X. Ruan, Y. Gao, H. Song, J. Yu, and D. Gong, "Robot attitude estimation based on kalman filter and application to balance control," *Advanced Science Letters*, vol. 6, no. 5, pp. 542–546, 2012.

[6] J. Vaganay, M. J. Aldon, and A. Fournier, "Mobile robot attitude estimation by fusion of inertial data," in *Proceedings of the IEEE International Conference on Robotics and Automation, ICRA'93*, pp. 277–282, 1993.

[7] S. M. Persson and I. Sharf, "Steady-state invariant Kalman filter for attitude and imbalance estimation of a neutrally-buoyant airship," in *Proceedings of the AIAA Guidance, Navigation, and Control Conference*, (Boston, Massachusetts), August 2013.

[8] H. G. de Marina, F. J. Pereda, J. M. Giron-Sierra, and F. Espinosa, "UAV attitude estimation using unscented kalman filter and triad," *IEEE Transactions on Industrial Electronics*, vol. 59, no. 11, pp. 4465–4474, 2011.

[9] J. M. Pflimlin, T. Hamel, and P. Souères, "Nonlinear attitude and gyroscope's bias estimation for a VTOL UAV," *International Journal of Systems Science*, vol. 38, pp. 197–210, June 2007.

[10] S. Khandenwal and C. Chevallereau, "Estimation of the trunk attitude of a humanoid by data fusion of inertial sensors and joint encoders," in *Proceedings of the IEEE Sixteenth International Conference on Climbing and Walking Robots, CLAWAR 2013*, (Sydney, Australia), pp. 822–830, July 2013.

[11] L. Wang, Z. Liu, C. Chen, Y. Zhang, S. Lee, and X. Chen, "A UKF-based predictable SVR learning controller for biped walking," *IEEE Transactions on Systems, Man, and Cybernetics*, vol. 43, pp. 1440–1450, November 2013.

[12] M. Bloesch, M. Hutter, M. Hoepflinger, S. Leutenegger, C. Gehring, C. D. Remy, and R. Siegwart, "State estimation for legged robots - consistent fusion of leg kinematics and IMU," in *Proceedings of Robotics: Science and Systems*, (Sydney, Australia), July 2012.

[13] H. Rehbinder and X. Hu, "Drift-free attitude estimation for accelerated rigid bodies," in *Proceedings of the IEEE International Conference on Robotics and Automation, ICRA'01*, pp. 4244–4249, 2001.

[14] S. P. N. Singh and K. J. Waldron, "Attitude estimation for dynamic legged locomotion using range and inertial sensors," in *Proceedings of the IEEE International Conference on Robotics and Automation, ICRA'05*, pp. 1663–1668, April 2005.

[15] G. Ligorio and A. M. Sabatini, "Extended Kalman filter-based methods for pose estimation using visual, inertial and magnetic sensors: Comparative analysis and performance evaluation," *Sensors*, vol. 13, pp. 1919–1941, 2013.

[16] A. M. Sabatini, "Variable-state-dimension Kalman-based filter for orientation determination using inertial and magnetic sensors," *Sensors*, vol. 12, pp. 8491–8506, 2012.

[17] B. Barshan and H. F. Durrant-Whyte, "Inertial navigation systems for mobile robots," *IEEE Transactions on Robotics and Automation*, vol. 11, pp. 328–342, June 1995.

[18] H. Rehbinder and X. He, "Nonlinear pitch and roll estimation for walking robots," in *Proceedings of the IEEE International Conference on Robotics and Automation, ICRA'00*, pp. 2617–2622, 2000.

[19] S. M. Persson and I. Sharf, "Invariant momentum-tracking Kalman filter for attitude estimation," in *Proceedings of the 2012 IEEE International Conference on Robotics and Automation, ICRA 2012*, (St. Paul, MN), pp. 592–598, May 2012.

[20] H. D. Taghirad, S. F. Atashzar, and M. Shahbazi, "Robust solution to three-dimensional pose estimation using composite extended Kalman observer and kalman filter," *ET Computer Vision*, pp. 1–13, 2011.

[21] F. Kanehiro, K. Fujiwara, S. Kajita, K. Yokoi, K. Kaneko, H. Hirukawa, Y. Nakamura, and K. Yamane, "Open architecture humanoid robotics platform," in *Proceedings of the 2002 IEEE International Conference on Robotics and Automation, ICRA 2002*, (Washingon, DC), pp. 24–30, May 2002.

[22] B. Siciliano, L. Sciavicco, L. Villani, and G. Oriolo, *Robotics: Modelling, Planning and Control*. Advanced Textbooks in Control and Signal Processing, Springer, second ed., 2009.

Paolo Pierro received his Laurea (BSc.) Degree and his Laurea Specialistica (MSc.) Degree in Electronic Engineering from the Universitat degli Studi di Salerno, Italy, in 2002 and 2005, respectively. In July 2009, he obtained his Master Degree in Robotics and Automation from the University Carlos III of Madrid, Spain, obtaining his Ph.D. Degree in 2012 from the same University. His research interests include human-humanoid collaboration and interaction and control of humanoid robots.

Concepción A. Monje received her MSc. Degree in Electronics Engineering from the Industrial Engineering School of the University of Extremadura, Spain, in 2001, and her Ph.D. Degree in Industrial Engineering from the University of Extremadura, Spain, in 2006. In September 2006 she joined the University Carlos III of Madrid as a Visiting Professor in the Department of Electronics and Electromechanical Engineering. Her research focuses on control theory and applications of fractional calculus in control systems and robotics. She has been working in these areas for over 8 years, and she has published over 50 technical papers mostly related to control and robotics.

Nicolas Mansard received the joint M.Eng. and M.Sc. degrees in robotics and image processing from the École Nationale Sup érieure d'Informatique et de Mathématiques Appliquées de Grenoble, Grenoble, France, and the University Joseph Fourier, Grenoble, and the Ph.D. degree for his work with the Lagadic Group, Institut National de Recherche en Informatique et en Automatique (INRIA), Rennes, France, in 2006. He spent one year with Stanford University, Stanford, CA, with O. Khatib and one year with the Joint Research Laboratory, National Institute of Advanced Industrial Science and Technologies, Japan, with A. Kheddar. He is currently with the GEPETTO Group, Laboratory for Analysis and architecture of Systems (LAAS), Centre National de la Recherche Scientifique (CNRS), University of Toulouse, Toulouse, France. His research is concerned with sensor-based robot animation.

Philippe Souères received the M.Sc. degree in Mathematics, the Ph.D. degree in Robotics, and the Habilitation degree, all from the University of Toulouse, Toulouse, France, in 1990, 1993, and 2001, respectively. From 1993 to 1994, he was with the Department of Electrical Engineering and Computer Science, University of California, Berkeley, with Prof. S. Sastry. Since then, he has been involved in different facets of robot perception and control with the Laboratory for Analysis and Architecture of Systems (LAAS), Centre National de la Recherche Scientifique (CNRS), University of Toulouse, Toulouse, France. Since 2003, he has been cooperating with neuroscientists on multisensory and sensorimotor integration. From 2006 to 2007, he was with the Brain and Cognition Research Center (UMR5549), Toulouse. Since 2008, he has been with the GEPETTO Group, LAAS-CNRS, where, since 2010, he has been leading the group. His research interests include control, robot vision and audio, wheeled and flying robots, humanoid systems, and neuroscience.

Carlos Balaguer received his Ph.D. in Automation from the Polytechnic University of Madrid (UPM), Spain, in 1983. From 1983-1994 he was with the Department of Systems Engineering and Automation of the UPM as Associated Professor. Since 1996, he has been a Full Professor of the RoboticsLab at the University Carlos III of Madrid. He is currently the Vicechancellor for research of the university. His research has included humanoid and assistive and service robots, among others. He participates in numerous EU projects since 1989, such as Eureka projects SAMCA, AMR and GEO, Esprit projects ROCCO and CEROS, Brite project FutureHome, IST project MATS, and the 6FP IP projects ManuBuild, I3CON, and Strep Robot@CWE. He has published more than 180 papers in journals and conference proceedings, and several books in the field of robotics.

AUTHORS' ADDRESSES

Paolo Pierro, Ph.D.
Prof. Concepción A. Monje, Ph.D.
Prof. Carlos Balaguer, Ph.D.
System Engineering and Automation Department,
Higher Polytechnic School,
University Carlos III of Madrid,
Avenida de la Universidad 30, 28911 Leganés,
Madrid, Spain.
email: ppierro@ing.uc3m.es, cmonje@ing.uc3m.es,
balaguer@ing.uc3m.es

Prof. Nicolas Mansard, Ph.D.
Prof. Philippe Soueres, Ph.D.
Laboratory of Analysis and Systems Architecture,
LASS-CNRS,
7 Avenue du Colonel Roche,
31077 Toulouse Cedex 4, France.
email: nicolas.mansard@laas.fr, soueres@laas.fr

Received: 2013-06-09
Accepted: 2015-01-27